

# Interlayer magnetic frustration driven quantum spin disorder in honeycomb compound $\text{In}_3\text{Cu}_2\text{VO}_9$

Da-Yong Liu<sup>1</sup>, Ying Guo<sup>1</sup>, Xiao-Li Zhang<sup>1</sup>, Jiang-Long Wang<sup>2</sup>, Zhi Zeng<sup>1</sup>, H. Q. Lin<sup>3</sup> and Liang-Jian Zou<sup>1\*</sup>

<sup>1</sup> Key Laboratory of Materials Physics, Institute of Solid State Physics,

Chinese Academy of Sciences, P. O. Box 1129, Hefei, Anhui 230031, China

<sup>2</sup> College of Physics Science and Technology, Hebei University, Baoding 071002, China

<sup>3</sup> Department of Physics, Chinese University of Hong Kong, Shatin, New Territory, Hong Kong, China

(Dated: May 18, 2021)

We present electronic and magnetic properties of a honeycomb compound  $\text{In}_3\text{Cu}_2\text{VO}_9$  in this paper. We find that the parent phase is a charge transfer insulator with an energy gap of about 1.5 eV. Singly occupied  $d_{3z^2-r^2}$  electrons of copper ions contribute an  $S = 1/2$  spin, while vanadium ions show nonmagnetism. Oxygen  $2p$  orbitals hybridizing with a small fraction of Cu  $3d$  orbitals dominate the density of states near  $E_F$ . The planar nearest-neighbor, next-nearest-neighbor and interplane superexchange couplings of Cu spins are  $J_1 \approx 16.2$  meV,  $J_2 \approx 0.3$  meV and  $J_z \approx 1.2$  meV, suggesting a low-dimensional antiferromagnet<sup>5</sup>. We propose that the magnetic frustration along the  $c$ -axis leads to a quantum spin disorder in  $\text{In}_3\text{Cu}_2\text{VO}_9$ , in accordance with the recent experiments.

PACS numbers: 71.20.-b, 75.10.Kt, 75.25.-j

## I. INTRODUCTION

Atoms in reduced dimensional lattice, for example, in two-dimensional (2D) honeycomb lattice, has low coordinate number and small spin number. Together with magnetic frustration, these electrons may experience strong spin fluctuations and probably form extremely low-dimensional (low-D) antiferromagnet (AFM), or even exotic spin liquid, quantum disorder, or quantum spin Hall state, so it has attracted great interest in recent theories<sup>1-13</sup>. A recent synthesized honeycomb compound  $\text{In}_3\text{Cu}_2\text{VO}_9$ <sup>14-16</sup> is such a system with reduced dimensionality and frustration. According to the chemical valence analysis, the copper ions with  $3d^9$  configuration contribute a spin-1/2 magnetic moment, while the  $3d$  orbitals in vanadium ions are empty and contribute no magnetic moment. Due to the large separation between Cu/V-O layers, the copper spins form a quasi-2D honeycomb lattice<sup>15</sup>. This compound exhibits unusual magnetic behavior: it shows neither an AFM long-range order in magnetic susceptibility measurement, nor any magnetic phase transition peak in specific heat data<sup>14,16</sup>. However, Zn or Co doping can induce a weak or strong three-dimensional (3D) AFM long-range order observed experimentally<sup>16</sup>. It inspires great interest in such a topic: whether the ground state of this compound is low-dimensional AFM, or spin liquid predicted by Meng *et al.*<sup>1</sup>.

Additionally, it is well known that noninteracting or weakly interacting electrons in hexagonal graphene is a typical example of *Dirac* fermions. It is not very clear that how the properties of Dirac fermions evolve with the increase of Coulomb interactions. Therefore,  $\text{In}_3\text{Cu}_2\text{VO}_9$  with hexagonal Cu ions is probably a realistic material to testify how the electronic correlations affect the *Dirac* fermions. In the meantime, through the magnetic susceptibility and specific heat measurements, it's hard to distinguish possible ground state between a low-dimensional

AFM and a spin liquid<sup>16</sup>. All of these drive us to explore the electronic properties and magnetism in  $\text{In}_3\text{Cu}_2\text{VO}_9$  by combining the first-principles electronic structure calculations and analytic methods, since it could provide us first insight to this compound.

Utilizing the local density functional (LDA) and the correlation correction approaches, together with the analytical perturbation method, we show that  $\text{In}_3\text{Cu}_2\text{VO}_9$  is an AFM charge transfer insulator with copper  $d_{3z^2-r^2}$  orbitals half filled and contributing  $S = 1/2$  spins. However, vanadium ions are nonmagnetic (NM). The oxygen  $2p$  orbitals dominate the density of states (DOS) near  $E_F$ . We extract not only tight-binding parameters between copper ions, but also various spin coupling strengths between Cu spins. Furthermore, we show that the absence of 3D AFM long-range order observed experimentally in  $\text{In}_3\text{Cu}_2\text{VO}_9$  arises from the magnetic frustration of Cu spins along the  $c$ -axis, leading to a quantum disorder phase. Meanwhile, in terms of this new scenario, we address the evolution of the magnetic properties on the Co and Zn dopings in  $\text{In}_3\text{Cu}_2\text{VO}_9$ , giving a plausible explanation of the experimental behavior. We also suggest the possibility that doping in oxygen sites may drive the system to a spin liquid or superconducting phase. The rest of this paper is organized as follows: in Sec. II, we briefly describe the unit cell of  $\text{In}_3\text{Cu}_2\text{VO}_9$  and numerical calculation methods; in Sec. III, we present the major numerical results and our analysis; Sec. IV is devoted to the remarks and conclusion.

## II. NUMERICAL METHODS

We first study the electronic state properties of the honeycomb compound  $\text{In}_3\text{Cu}_2\text{VO}_9$  by employing the first-principles electronic structure calculation approach so as to elucidate its groundstate properties. The electronic structure calculations were performed using the

self-consistent full potential linearized augmented-plane-wave (FP-LAPW) scheme in the WIEN2K programme package.<sup>17</sup> We used 36  $k$  points in the irreducible part of the first Brillouin zone. The muffin-tin sphere radii were selected to be 2.36, 1.93, and 1.71 a.u. for In, Cu (V), and O in  $\text{In}_3\text{Cu}_2\text{VO}_9$ . The plane-wave cutoff parameter  $R_{MT}K_{max}$  was 7.0, and the cutoff between the core and valence states was  $-7.0$  Ry in all calculations. Exchange and correlation effects were taken into account in the generalized gradient approximation (GGA) by Perdew, Burk, and Ernzerhof (PBE)<sup>18</sup>. In order to explicitly take into account the correlated effect of the  $3d$  electrons of Cu (V) ions, we also performed GGA+ $U$  calculations for  $\text{In}_3\text{Cu}_2\text{VO}_9$ . The effective Coulomb interaction  $U_{eff} = U - J_H$  ( $U$  and  $J_H$  are the on-site Coulomb interaction and the Hund's rule coupling, respectively) was used instead of  $U$ . We take  $U_{eff} = 8.0$  eV for copper and 4.0 eV for vanadium according to the similar compounds<sup>19-21</sup>.

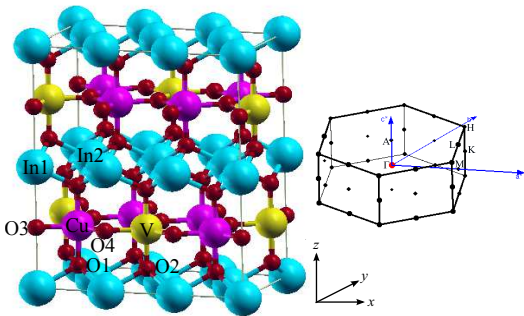


FIG. 1. (Color online) (a) Unit cell of  $\text{In}_3\text{Cu}_2\text{VO}_9$  ( $Cmcm$  space group), and corresponding high symmetry points in the first Brillouin zone.

To model the low-energy process in  $\text{In}_3\text{Cu}_2\text{VO}_9$ , the tight-binding parameters in the NM (or paramagnetic (PM)) phase are necessary. We also perform the local density functional (LDA) calculations for NM  $\text{In}_3\text{Cu}_2\text{VO}_9$ . The NM band structures of  $\text{In}_3\text{Cu}_2\text{VO}_9$  are obtained by using the full-potential linearized augmented plane-wave plus local orbitals (FP-LAPW+lo) scheme implemented in the WIEN2K package<sup>17</sup>. In order to compare our numerical results with the experimental data, we adopt the experimental structural data of  $\text{In}_3\text{Cu}_2\text{VO}_9$  measured by neutron powder diffraction<sup>14</sup>. This compound has an orthorhombic structure with space group  $Cmcm$  and lattice constants  $a = 10.0491$  Å,  $b = 5.8019$  Å, and  $c = 11.8972$  Å, as shown in Fig. 1. It was found that  $\text{In}_3\text{Cu}_2\text{VO}_9$  has a honeycomb layered structure with Cu atoms forming hexagonal net and V atoms in the center of an hexagon. A Cu atom is surrounded by five O atoms in a trigonal bipyramidal environment. Detailed results of band structure are addressed in what follows.

## A. Nonmagnetic State

We first present the NM electronic structures of  $\text{In}_3\text{Cu}_2\text{VO}_9$  in Fig. 2. It shows that the major orbital character of the band structures near  $E_F$  is a  $3z^2 - r^2$  symmetry of copper  $3d$  orbitals. This Cu  $3d_{3z^2-r^2}$  orbital in the honeycomb lattice, similar to the  $p_z$  orbital of carbon in graphene, contributes an outstanding property of the band structures, *i.e.*, a *Dirac* cone with the approximately linear spectrum is observed around the  $H$  point, as seen in Fig. 2. The linear energy spectrum ranges from  $-0.2$  to  $0.2$  eV. We notice that the original *Dirac* point around the  $K$  points opens a small energy gap, about 0.2 eV, also as seen in Fig. 2, which is attributed to the weak interlayer coupling between Cu/V-O hexagonal planes. Though parts of empty V  $3d$  orbital

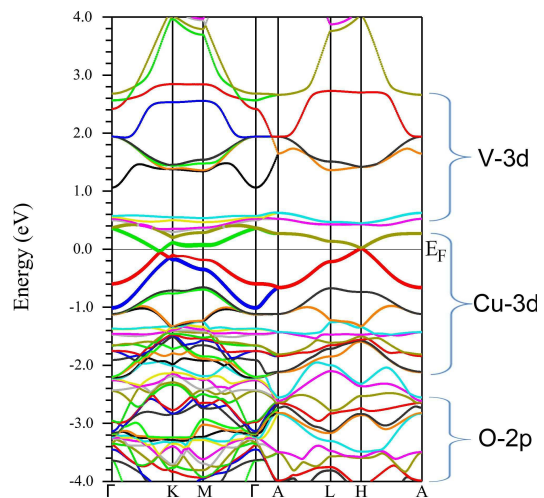


FIG. 2. (Color online) Band structures with orbital character of  $\text{In}_3\text{Cu}_2\text{VO}_9$  in the NM situation by the LDA method. We indicate the major orbital component of each band. The bands marked with heavy lines are Cu  $3d_{3z^2-r^2}$  orbitals.

are near the top of Cu  $3d_{3z^2-r^2}$  orbitals, they do not directly hybridize with each other considerably. A part of filled oxygen  $2p$  orbitals are close to the bottom of Cu  $3d_{3z^2-r^2}$  orbitals, and these  $2p$  orbitals also do not considerably mix with  $3d_{3z^2-r^2}$  orbitals, as we see the partial density of states (PDOS) of  $\text{In}_3\text{Cu}_2\text{VO}_9$  in Fig. 3. Thus the low-energy physics in  $\text{In}_3\text{Cu}_2\text{VO}_9$  could be approximately described by the Cu  $3d_{3z^2-r^2}$  orbitals across  $E_F$ .

Based on the fact that Cu  $3d_{3z^2-r^2}$  orbitals mainly distribute from  $-1.0$  eV to  $0.4$  eV, we extract these four Cu  $3d_{3z^2-r^2}$  bands (notice that we have four Cu atoms in primitive cell) from the full band structures and fit these bands with a single-orbital tight-binding model with the nearest-neighbor (NN), next NN (NNN) and  $3rd$  NN hopping integrals in the Cu/V-O plane and between the planes. These tight-binding parameters are listed in Table I. Notice that the LDA methods deal with the NM state rather than the PM one. But as we know, the over-

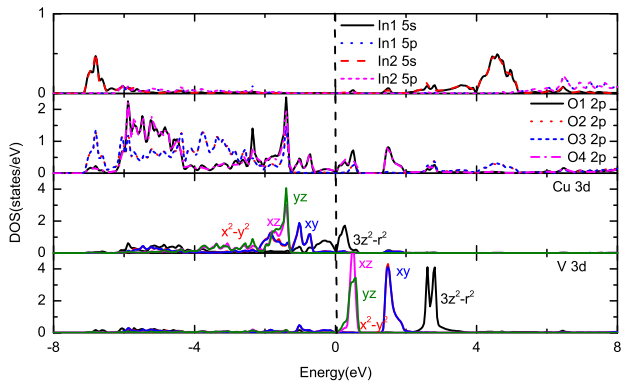


FIG. 3. (Color online) Partial density of states (PDOS) of  $\text{In}_3\text{Cu}_2\text{VO}_9$  in the NM situation by the LDA method.

lap and hopping integrals of electrons depend on the spatial wavefunctions, and are independent of the spin degree of freedom. Thus the hopping parameters obtained in the NM state are the same to those in the PM state. One can easily find that the intraplane NN hopping integral  $t_1$  is about 7.5, 31 and 3.7 times of the intraplane NNN hopping  $t_2$ , 3rd hopping  $t_3$  and the interplane NN hopping  $t_c$ , respectively, suggesting the NN hopping and NN spin coupling dominate the transfer process and magnetic correlations in the ground state of  $\text{In}_3\text{Cu}_2\text{VO}_9$ .

### B. Degenerate Antiferromagnetic States

To understand the magnetism and insulating nature of undoped compound, we further adopt the spin-polarized GGA and correlation-corrected GGA+ $U$  schemes to uncover the groundstate properties of strongly correlated  $\text{In}_3\text{Cu}_2\text{VO}_9$ . We consider five kinds of different magnetic configurations, NM, ferromagnet (FM), A-type AFM (*i.e.*, interlayer AFM and intralayer FM), and G1- and G2-type AFM as the possible candidate ground state. Here G1- and G2-type AFM configurations shown in Fig. 6 are two different magnetic structures, both of which are derived from a conventional G-type AFM. In comparison with the G1-type AFM structure, the lower Cu/V-O hexagon (or Cu/V-O layer) in the G2-type structure rotates  $\pi/3$  degree. Thus the G1-type spin configuration

TABLE I. Tight-binding parameters  $t_\alpha$  and superexchange spin coupling strengths  $J_\alpha$  in  $\text{In}_3\text{Cu}_2\text{VO}_9$ . Subscripts 1, 2, 3 and  $c$  represent the NN, NNN, 3rd NN hopping integrals or spin coupling strengths in the planes, and the NN ones between the planes, respectively. All the energies are measured in units of meV.

$t_1$	$t_2$	$t_3$	$t_c$	$J_1$	$J_2$	$J_c$
-180.2	-24.1	5.8	-48.9	16.2	0.3	1.2

differs from the G2-type one. Our GGA+ $U$  numerical results show that the total energy of the NM state is the highest, and that of the G1- and G2-type AFM states are the lowest. Interestingly, we find that the G1- and G2-type AFM states are degenerate. This arises from the interlayer magnetic frustration of Cu spins, as will be discussed in detail later. The total energy difference between the FM and A-type AFM configurations is rather small. The energy difference between the lowest G1(G2)-type AFM and the second lowest A-type AFM or FM states is about 58.5 meV, suggesting that the AFM magnetic couplings between Cu spins in  $\text{In}_3\text{Cu}_2\text{VO}_9$  are dominant.

To examine the effect of the on-site Coulomb interaction parameter  $U$  on the calculation results, we also perform the spin-polarized GGA calculations for the purpose of comparison. The PDOS of  $\text{In}_3\text{Cu}_2\text{VO}_9$  for G1(G2)-type AFM state is shown in Fig. 4. It is found that

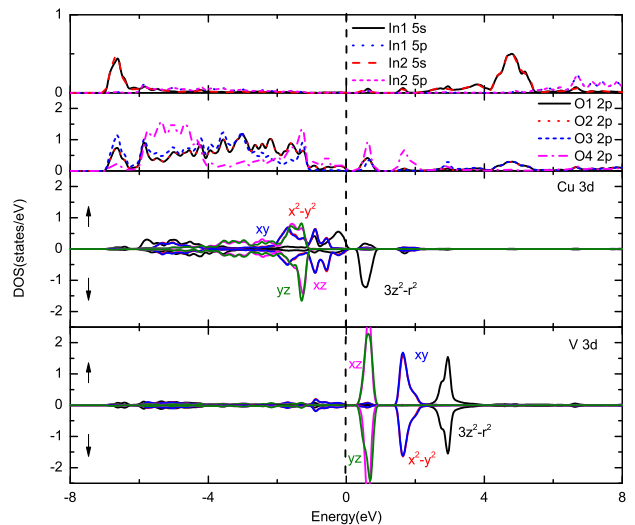


FIG. 4. (Color online) PDOS of  $\text{In}_3\text{Cu}_2\text{VO}_9$  for G1(G2)-type AFM state by the spin-polarized GGA method.

the system is an insulator with an energy gap of 0.4 eV. However the calculated magnetic moment is only  $0.4 \mu_B$ , smaller than that observed by the experiment, about  $0.5 \mu_B$ <sup>14</sup>. Considering the fact that the LSDA results usually overestimate the magnitude of a magnetic moment, while the experimental results underestimate it due to the significant disorder and fluctuations in realistic compounds, one can expect that there exists a larger magnetic moment than  $0.5 \mu_B$ . In a similar system  $\text{Cu}_2\text{V}_2\text{O}_7$  with  $0.73 \mu_B$  for  $U_{eff} = 6.52$  eV<sup>19</sup>, the GGA+ $U$  calculations are also needed for  $\text{In}_3\text{Cu}_2\text{VO}_9$ . We choose the Coulomb parameters lying in a physical parameter range for  $\text{In}_3\text{Cu}_2\text{VO}_9$ , *i.e.*  $U_{eff} = 8$  eV for Cu ions, and 4 eV for V ions according to the similar compounds, such as  $\text{Cu}_2\text{V}_2\text{O}_7$ <sup>19</sup> and  $\text{In}_2\text{VO}_5$ <sup>20</sup>, as well as the general compounds, such as cuprates and vanadium oxides ( $\text{V}_2\text{O}_3$ <sup>21</sup>), *etc.*. Notice that we perform the numerical calculations for several different Coulomb parameters for Cu and V

atoms to systematically investigate their influence on our results, *i.e.*  $U_{eff} = 6 \sim 8$  eV for Cu<sup>19</sup> and  $U_{eff} = 3 \sim 5$  eV for V<sup>20,21</sup>. From our numerical calculations, we find that the band gap and the magnetic moment vary from 1.37 to 1.5 eV and from 0.72 to 0.79  $\mu_B$ , respectively, when  $U_{eff}$  changes from 6 to 8 eV for Cu and from 3 to 5 eV for V. This clearly shows that the electronic and magnetic properties do not crucially depend on the values of the parameter  $U$  in the physical range.

To further uncover the insulating character of  $\text{In}_3\text{Cu}_2\text{VO}_9$ , the PDOS for G1(or G2)-type AFM state by the GGA+ $U$  approach is plotted, as seen in Fig. 5. The system is obviously an insulator with an energy gap of 1.5 eV. We found that oxygen  $2p$  orbitals consist of the major bands near  $E_F$ , ranging from 0 to  $-4.0$  eV. While the gravity center of Cu  $3d$  orbitals lie far from  $E_F$ . The center of the spin-up  $3d$  orbital lies at about  $-5.9$  eV, and that of the spin-down  $3d$  orbitals lies at about  $-4.8$  eV. This gives rise to the exchange splitting of Cu  $3d$  orbitals about  $\Delta_{ex} \approx 1.1$  eV, implying that the Hund's rule coupling  $J_H = \Delta_{ex}/2S \approx 1.1$  eV. Such a large exchange splitting also shows a strong Coulomb correlation on Cu  $3d$  orbitals. Note that the charge transfer energy between O  $2p$  orbital and Cu  $3d$  orbital in  $\text{In}_3\text{Cu}_2\text{VO}_9$ ,  $\Delta = \epsilon_{2p} - \epsilon_{3d}$ , which has the same order as the insulating energy gap, is considerably smaller than the on-site Coulomb interaction of Cu  $3d$  electrons, demonstrating that  $\text{In}_3\text{Cu}_2\text{VO}_9$  is a charge transfer insulator.

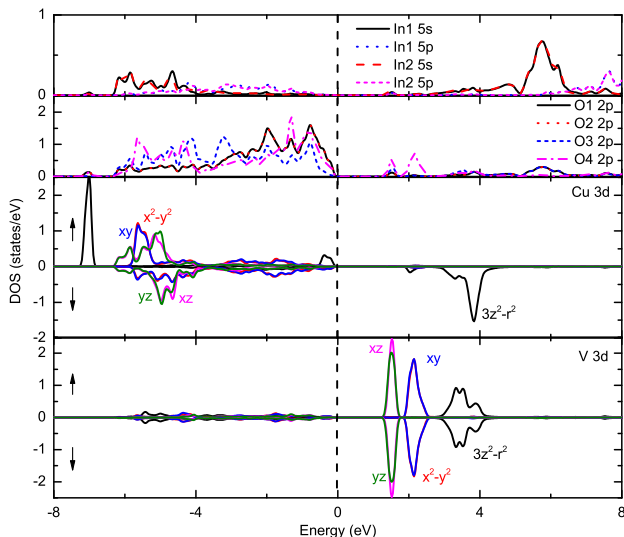


FIG. 5. (Color online) PDOS of  $\text{In}_3\text{Cu}_2\text{VO}_9$  for G1(G2)-type AFM state by the spin-polarized GGA+ $U$  method.

The charge distribution and occupation numbers in the  $3d$  orbitals of Cu and V are essential to understand the electronic properties of  $\text{In}_3\text{Cu}_2\text{VO}_9$ . Our results show that in the Cu  $3d$  orbitals, the hole mainly occupies the active  $d_{3z^2-r^2}$  orbital. It has a total number of 1.17 electrons, or 0.83 holes, in the  $d_{3z^2-r^2}$  orbital. In contrary to the chemical valence analysis, V has totally 1.87 electrons in its  $3d$  orbitals, though it shows NM or no spin polar-

ization in the present GGA+ $U$  ansatz. This arises from a strong  $p$ - $d$  hybridization between V and O atoms, and a fraction of electrons transfer from oxygen  $2p$  orbitals to vanadium  $3d$  orbitals.

Fig. 5 displays that the main DOS of copper lies from  $-7$  eV to  $-4$  eV, though a tiny portion of  $3d$  electrons lie between  $-4$  eV to  $E_F$  which arises mainly from the hybridization of Cu  $3d$  orbital with the  $2p$  orbitals near  $E_F$  of surrounding O anions. It's observed from Fig. 5 that the  $3d_{3z^2-r^2}$  orbital in Cu is almost fully spin polarized. The magnetic moment of Cu spin is almost contributed from the well localized spin-up  $3d_{3z^2-r^2}$  orbital at the position of about 7 eV below  $E_F$ . We find that the orbital ground state is the Cu  $3d_{3z^2-r^2}$  character, in agreement with the electron spin resonance experiment by Kataev *et al.*<sup>22</sup>.

Meanwhile, a small but finite DOS distributed from  $-6$  eV to  $E_F$  is seen in V  $3d$  orbitals, showing that the two  $3d$  electrons form a wide energy band below the Fermi energy. Obviously, other V  $3d$  electrons contribute the highest empty conduction bands, as we see in Fig. 5. The PDOS of V shows that two  $3d$  electrons in V are not spin polarized and allocate in five  $3d$  orbitals with almost equal weight, in sharp contrast to those of Cu atoms. Fig. 5 shows that In  $5p$  orbitals give rise to a small DOS in a wide energy range. In contrast, the DOS of oxygen mainly distributes near  $E_F$  and is greatly larger than that of In. Such a strongly correlated character in  $\text{In}_3\text{Cu}_2\text{VO}_9$  is similar to that in the parent phases of high- $T_c$  cuprates. This implies that the doping in O sites can readily affect the transport properties in  $\text{In}_3\text{Cu}_2\text{VO}_9$ , and easily drive the system transit to metallic or superconducting phase once hole carriers are doped in oxygen  $2p$  bands.

### C. Magnetic Coupling Strengths

The groundstate magnetic properties of  $\text{In}_3\text{Cu}_2\text{VO}_9$  is the central issue of this paper. As described above, our numerical results demonstrate that the stablest phase is the degenerate G1- and G2-type AFM states. The magnetic moment mainly contributes from copper spins with a total net magnetic moment of 0.79  $\mu_B$  per Cu atom in which the average electron number is 0.98 in the spin-up band, and 0.19 in the spin-down one. The magnetic moment mainly arises from the  $d_{3z^2-r^2}$  orbital of copper. Apparently, a strong electron correlation and a large Hund's rule coupling result in such a large spin polarization, leading to a well defined local moment in coppers. In contrast, vanadium is NM, though it is  $3d^2$  configuration with two electrons distributing from  $E_F$  to  $-7.0$  eV. Its NM character may arise from the strong  $p$ - $d$  hybridization between V and O, resulting in a weak correlation between V  $3d$  electrons. We do not rule out the possibility of spin frustrations in the present Cu-V geometry, which may deserve further discussion in the future. Due to the full fillings of the oxygen  $2p$  orbitals and In  $5p$  orbitals, both O and In are not spin polarized.

The insulating nature in  $\text{In}_3\text{Cu}_2\text{VO}_9$  suggests that the local spins of coppers interact through a superexchange couplings mediated via oxygens and vanadium. One expects that the contributions to the NN and NNN Cu-Cu superexchange couplings arise from the direct hopping between  $d_{3z^2-r^2}$  electrons, the indirect hopping between Cu spins through the  $p-d$  hybridization of intermediate oxygen anions and through the O-V-O bridge. To quantitatively obtain the superexchange coupling strengths, we utilize the tight-binding parameters obtained in Table I to estimate the NN and NNN superexchange couplings between Cu spins in the Cu/V-O plane and between the planes, taking the effective Coulomb interaction  $U$  as 8 eV. A  $t/U$  expansion of the Hubbard model is used to obtain an effective  $J_1$ - $J_2$ - $J_c$  spin  $S=1/2$  model on a honeycomb lattice:

$$H = J_1 \sum_{\langle ij \rangle_{ab}} \vec{S}_i \cdot \vec{S}_j + J_2 \sum_{\langle\langle ij \rangle\rangle_{ab}} \vec{S}_i \cdot \vec{S}_j + J_c \sum_{\langle ij \rangle_c} \vec{S}_i \cdot \vec{S}_j, \quad (1)$$

where  $J_1 = 4t_1^2/U - 16t_1^4/U^3$ ,  $J_2 = 4t_2^2/U + 4t_1^4/U^3$  and  $J_c = 4t_c^2/U$  are the NN, NNN intralayer and the NN interlayer magnetic couplings, respectively. We find that the intraplane and interplane NN superexchange couplings are about  $J_1 \approx 16.2$  meV and  $J_c \approx 1.2$  meV, respectively; and the intraplane NNN superexchange couplings are about  $J_2 \approx 0.3$  meV. More long-range spin couplings are so small to be negligible. This gives rise to  $J_2/J_1 \approx 0.02$ , in addition to a rather weak interlayer coupling of  $J_c/J_1 \approx 0.07$ . All of these spin coupling strengths have been listed in Table I. From the literature available, we find that the spin coupling strengths of  $\text{In}_3\text{Cu}_2\text{VO}_9$  fall in the parameter range of a 2D Heisenberg AFM<sup>5,25</sup>, showing that  $\text{In}_3\text{Cu}_2\text{VO}_9$  is an insulator with 2D AFM. As we will illustrate later, such a weak interlayer magnetic coupling and the spin frustration prevent from the long-range AFM order in  $\text{In}_3\text{Cu}_2\text{VO}_9$ .

### III. REMARKS AND CONCLUSIONS

It is observed experimentally that neither the specific heat nor magnetic susceptibility exhibits AFM-PM transition<sup>16</sup>: the former is almost  $T^2$  dependent, and the latter linearly increases with the lift of temperature. Consequently, one naturally suspects that the ground state of  $\text{In}_3\text{Cu}_2\text{VO}_9$  might be a gapless spin liquid phase, a long-time searched exotic quantum phase both theoretically and experimentally, since such a phase in *Kagome* lattice also demonstrates similar unusual temperature-dependent behavior in the low T regime<sup>3,23</sup>. Meanwhile, a strongly low-D AFM may exhibit similar behaviors<sup>24</sup>. Though both a low-dimensional AFM and a spin liquid have local permanent magnetic moments, and do not display any sign of ordering in specific heat and magnetic susceptibility down to the lowest temperatures despite of

comparable strong AFM interactions. A low-dimensional AFM could be different from a spin liquid in many aspects. For example, a 2D AFM has a long-range correlation and long-range order at  $T=0$  K as well as short-range one at finite T, while a spin liquid only has short-range correlation, even at  $T=0$  K; this leads to distinct low-temperature behavior in magnetic susceptibility for a 2D AFM and a spin liquid, *etc.*. Therefore our theoretical analysis above suggests 2D AFM ground state rather than a spin liquid, though it is still mysterious why  $\text{In}_3\text{Cu}_2\text{VO}_9$  exhibits neither an AFM long-range order in the low temperature regime nor a Curie-Weiss law in the high temperature regime<sup>14,16</sup>, which is exotic and distinctly different from undoped cuprates.

An earlier experimental study by Möller *et al.*<sup>14</sup> attributed the absence of a 3D AFM long-range order to the disorder stacking of 2D Cu/V order domains along the  $c$ -axis. However, from our preceding data and the particular geometry of  $\text{In}_3\text{Cu}_2\text{VO}_9$ , as an alternative explanation, we propose that it is the strong AFM frustration along the  $c$ -axis leads to the absence of the 3D AFM long-range order in  $\text{In}_3\text{Cu}_2\text{VO}_9$ . As seen the Cu-V geometric configuration among two Cu-V layers in Fig. 6, a Cu spin has two NN layers along the  $c$ -axis, it has

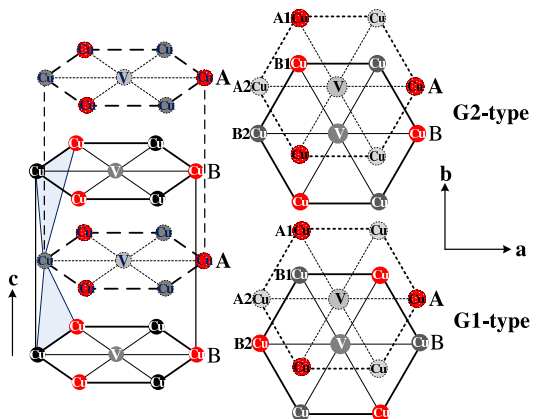


FIG. 6. (Color online) Schematics of frustrated magnetic configurations of Cu spins between A and B layers (left panel), and a top view of the G1(G2)-type AFM (right panel). A Cu spin in the upper layer (dash line) has the same distance to two Cu spins in the lower layer (solid line), consisting of an isosceles triangle. Filled gray and red circles represent spin down and spin up, respectively.

the same distance to other two Cu spins in the upper or lower layer, forming an isosceles triangle which is a notorious spin configuration with magnetic frustration. Our analysis above has shown that both the spin couplings of the interlayer and intralayer spins are AFM, indicating the spin fluctuations along the  $c$ -axis will be very large. Thus in  $\text{In}_3\text{Cu}_2\text{VO}_9$  the intralayer Cu spins are AFM correlated, while the interlayer Cu spins are quantum disordered. Such a frustration scenario could unifiedly account for both the presence of low-D AFM correlation<sup>15</sup> and the absence of 3D AFM order<sup>14,16,22</sup> in

recent experiments.

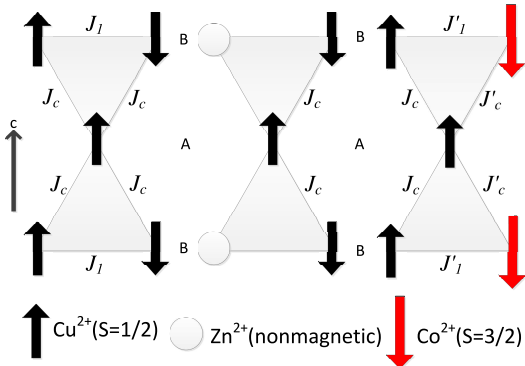


FIG. 7. (Color online) Schematics of the frustration scenario to explain the evolution of the magnetic behavior in Zn- and Co-doped  $\text{In}_3\text{Cu}_2\text{VO}_9$ .

Furthermore, we apply our frustration scenario to uncover the evolution of the magnetic properties on the Co and Zn dopings in  $\text{In}_3\text{Cu}_2\text{VO}_9$ , giving a possible explanation of the experimental behavior, as shown in Fig. 7. The Zn and Co dopings break the inter-layer frustration, while the NM  $\text{Zn}^{2+}$  ions destroy the intra-layer AFM. On the contrary, high spin-3/2  $\text{Co}^{2+}$  ions enhance it. Thus the Zn doping induces a weak AFM at low doping, but suppresses the AFM state completely at high doping. In comparison, the Co doping results in a strong AFM with large effective magnetic moment. All the results are in accordance with the experimental observations.

Moreover, as we point out above, the hole doping in O sites of  $\text{In}_3\text{Cu}_2\text{VO}_9$  may introduce carriers near Fermi energy. With the increase of carriers, one expects that the screening effect can greatly reduce the Coulomb interaction, and weaken the electronic correlation. This may drive the  $\text{In}_3\text{Cu}_2\text{VO}_9$  system from an AFM ground state to a spin liquid phase<sup>1</sup>, since in the intermediate

correlation regime, a half-filled Hubbard system with the honeycomb structure exists a spin-liquid ground state<sup>1,4</sup>. Nevertheless, we don't expect that doped  $\text{In}_3\text{Cu}_2\text{VO}_9$  will form the well-known Zhang-Rice singlet in the Cu-O plane of cuprates, since the latter arises from the hybridization between Cu  $3d_{x^2-y^2}$  and O  $2p$  orbitals, forming delocalized states in the  $xy$  plane; while in the former, the  $3d_{3z^2-r^2}$  orbital mixes with O  $2p$  orbital, forming a delocalized state in the  $z$ -direction. This results in completely different transport properties in doped compounds, as Yan *et al.* observed in  $\text{In}_3\text{Cu}_{2-x}\text{Co}_x\text{VO}_9$  and  $\text{In}_3\text{Cu}_{2-x}\text{Zn}_x\text{VO}_9$ <sup>16</sup>.

In summary, the investigation of the electronic structure and magnetic properties in quasi-2D honeycomb compound  $\text{In}_3\text{Cu}_2\text{VO}_9$  demonstrates that the undoped phase is a charge transfer insulator with a gap of 1.5 eV, and oxygen  $2p$  orbitals dominate the bands near  $E_F$ . Spin-1/2 local moment antiferromagnetically interacts and occupies the  $3z^2-r^2$  orbital in copper. In contrast, the NM V ions have two electrons in the  $3d$  orbitals. The tight-binding parameters and estimated spin coupling strengths suggest that  $\text{In}_3\text{Cu}_2\text{VO}_9$  is a strongly 2D *Néel* AFM. We propose that the spin fluctuations arising from the magnetic frustration along the  $c$ -axis destroy the 3D AFM long-range order, leading to random stacking of Cu-V layers.

## ACKNOWLEDGMENTS

We acknowledge X. H. Chen provides us with original experimental data. This work was supported by the National Sciences Foundation of China under Grant No. 11074257 and 11104274, and Knowledge Innovation Program of the Chinese Academy of Sciences. Numerical calculations were performed at the Center for Computational Science of CASHIPS.

\* Corresponding author; zou@theory.issp.ac.cn

<sup>1</sup> Z. Y. Meng, T. C. Lang, S. Wessel, F. F. Assaad, and A. Muramatsu, *Nature* **464**, 847 (2010).

<sup>2</sup> S. M. Yan, D. A. Huse, and S. W. White, *Science* **332**, 1173 (2011).

<sup>3</sup> S. Saremi and P. A. Lee, *Phys. Rev. B* **75**, 165110 (2007).

<sup>4</sup> A. Vaezi and X.-G. Wen, arXiv:1010.5744; arXiv:1101.1662.

<sup>5</sup> B. K. Clark, D.A. Abanin, and S. L. Sondhi, *Phys. Rev. Lett.* **107**, 087204 (2011).

<sup>6</sup> F. Wang, *Phys. Rev. B* **82**, 024419 (2010).

<sup>7</sup> A. Liebsh, *Phys. Rev. B* **83**, 035113 (2011).

<sup>8</sup> J. He, S.-P. Kou, Y. Liang and S.-P. Feng, *Phys. Rev. B* **83** 205116 (2011); *ibid.*, **84**, 035127 (2011).

<sup>9</sup> Y.-M. Lu and Y. Ran, *Phys. Rev. B* **84**, 024420 (2011).

<sup>10</sup> H. H. Zhao, Q. N. Chen, Z. C. Cai, M. P. Qin, G. M. Zhang, and T. Xiang, arXiv:1105.2716.

<sup>11</sup> W.-S. Wang, Y.-Y. Xiang, Q.-H. Wang, F. Wang, F. Yang, and D.-H. Lee, *Phys. Rev. B* **85**, 035412 (2012).

<sup>12</sup> W. Wu, S. Rachel, W.-M. Liu, and K. Le Hur, arXiv:1106.0943.

<sup>13</sup> T. Li, *Euro. Phys. Lett.* **97**, 37001 (2012).

<sup>14</sup> A. Möller, U. Löw, T. Taetz, M. Kriener, G. Andre, F. Damay, O. Heyer, M. Braden, and J. A. Mydosh, *Phys. Rev. B* **78**, 024420 (2008).

<sup>15</sup> M. Yehia, E. Vavilova, A. Möller, T. Taetz, U. Löw, R. Klingeler, V. Kataev, and B. Büchner, *Phys. Rev. B* **81**, 060414(R) (2010).

<sup>16</sup> Y.-J. Yan, Z.-Y. Li, T. Zhang, X.-G. Luo, G.-J. Ye, Z.-J. Xiang, P. Cheng, L.-J. Zou, and X. H. Chen, *Phys. Rev. B* **85**, 085102 (2012).

<sup>17</sup> P. Blaha, K. Schwarz, G. Madsen, D. Kvasnicka, and J. Luitz: "Computer Code WIEN2k, an augmented plane wave plus local orbitals program for calculating crystal properties", Karlheinz Schwarz, Technische Universität

- Wien, Austria, (2001).
- <sup>18</sup> J. P. Perdew, K. Burke, and M. Ernzerhof, *Phys. Rev. Lett.* **77**, 3865 (1996).
- <sup>19</sup> M. Yashima, and R. O. Suzuki, *Phys. Rev. B* **79**, 125201 (2009).
- <sup>20</sup> H. Wang, and U. Schwingenschlögl, *J. Phys. Condens. Matter* **22**, 416002 (2010).
- <sup>21</sup> F. Rodolakis, P. Hansmann, J.-P. Rueff, A. Toschi, M. W. Haverkort, G. Sangiovanni, A. Tanaka, T. Saha-Dasgupta, O. K. Andersen, K. Held, M. Sikora, I. Alliot, J.-P. Itié, F. Baudelet, P. Wzietek, P. Metcalf, and M. Marsi, *Phys. Rev. Lett.* **104**, 047401 (2010).
- <sup>22</sup> V. Kataev, A. Möller, U. Löw, W. Jung, N. Schittner, M. Kriener, and A. Freimuth, *J. Magn. Magn. Mater.* **290-291**, 310 (2005).
- <sup>23</sup> Y. Ran, M. Hermele, P. A. Lee, X.-G. Wen, *Phys. Rev. Lett.* **98**, 117205 (2007).
- <sup>24</sup> K. Oka, I. Yamada, M. Azuma, S. Takeshita, K. H. Satoh, A. Koda, R. Kadono, M. Takano, and Y. Shlmakawa, *Inorg. Chem.* **47**, 7355 (2008).
- <sup>25</sup> F. Mezzacapo and M. Boninsegni, *Phys. Rev.* **85**, 060402 (2012).